Experimental Characterization of a Solar Combisystem with Seasonal Storage for a Single Detached House

Curtis Meister[1] and Ian Beausoleil Morrison[1]

[1] Carleton University, Ottawa (Canada)

Abstract

A solar combisystem with seasonal thermal energy storage has been designed and installed at the Urbandale Centre for Home Energy Research in Ottawa, Ontario, Canada. The system features a 28 m^2 evacuated tube solar array, 1350 litres of diurnal heat storage tanks, and a 37 m^3 buried water tank for seasonal heat storage. The single-detached research house is warmed through radiant floors supplied by either the diurnal or seasonal storage tanks, and domestic hot water is supplied with the diurnal tanks. This research aims to determine the performance of such a system over a full-scale one-year experiment, with the goal of demonstrating a high solar fraction. Preliminary results show that heat losses from the seasonal store exceed those expected from design values. Future experiments are identified.

Keywords: Solar thermal, solar combisystems, seasonal storage, solar domestic hot water

1. Introduction

The majority of energy consumed in cold-climate homes is used for space heating and domestic hot water (DHW). Our reliance on fossil fuels in the residential sector could be drastically reduced by replacing conventional space and hot water heating systems with solar combisystems. Solar combisystems provide space heating and hot water through solar-thermally-charged hot water storage tanks. Combisystems equipped with diurnal thermal energy storage (DTES) can be expected to achieve solar fractions (the fraction of energy demands met with solar energy alone) of 50-60% (Dincer and Rosen (2011), Edwards (2014)). For combisystems to achieve solar fractions approaching 100%, they will almost certainly require long term energy storage.

The focus of this research is an experimental facility equipped with a solar combisystem and seasonal storage in the form of a 37 m^3 buried water tank. In this paper, we describe the full-scale experiment that has been developed for this system and report on findings from preliminary heat loss tests. A high-level overview of the facility is given, followed by a detailed description of the system's instrumentation and control system. Finally, preliminary results of heat losses from the STES tank are presented and discussed.

a) b)

Fig. 1: a) The Urbandale Centre for Home Energy Research and b) installation of the seasonal storage tank

doi:10.18086/swc.2017.29.08 Available at http://proceedings.ises.org

2. Past Studies on Seasonal Storage

Thermal energy storage (TES) was studied extensively under Tasks 7 and 32 of the IEA (International Energy Agency) SHC (Solar Heating and Cooling) program. The programs explored many methods of thermal energy storage, including sensible, chemical and latent heat storage. Pinel et al. (2011) presented a comprehensive review of these methods for seasonal thermal energy storage, and concluded that for residential applications, sensible heat storage was currently the simplest, most cost effective and best-understood method. Indeed, most installed STES systems are simple sensible heat stores, using water or earth as a storage medium. This section briefly summarizes the relevant work in this area, particularly studies relating to STES for single homes.

2.1 Simulation Studies on Seasonal Storage

Simulation studies on STES have typically aimed to determine the optimum size of components in a solar combisystem with STES (array size, STES size). Sillman (1981) conducted simulation studies on buildings with long term heat storage, and determined that solar fractions increased with storage volume up until the “point of unconstrained operation”, when all excess solar gained could be stored. Braun et. al (1981)’s simulations agreed that increasing STES volume for a constant array size led to higher solar fractions until all collected heat could be stored. Wills (2013) looked at larger STES tank volumes (80-130 m^3 for single detached homes) than the latter two studies, and found that larger tank volumes decreased solar fractions due to the lower quality of energy (exergy) that could be stored. Kemery (2017) simulated the as-built combisystem and STES tank presented in this study, and found that a high solar fraction (over 90%) could be achieved.

Losses from seasonal stores have been consistently identified as a source of uncertainty in STES models. This is largely due to the complexity involved in simulating the ground domain. Some tank models (TRNSYS Type 534, Thermal Energy System Specialists (2017)) take a simplified approach, imposing a constant boundary temperature on the tank’s exterior wall. Other models, like those employed by Ochs (2009), Marazella(), and Wills (2013) employ 2D or 3D finite differencing to represent the ground temperature distribution. Pinel et al. (2011) point to a lack of consideration of a number of factors in ground heat transfer: humidity diffusion in soil, thermal coupling between the storage and house, and uncertainty in ground surface conditions. There are also uncertainties in the selection of material properties for models, particularly the thermal conductivity of insulating materials. This is treated in the next section.

2.2 Experimental Studies

Experimental facilities equipped with seasonal storage have mostly been limited to district scale systems, such as the heating system in Hannover, Germany (Ochs(2009), Raab(2005)) and Drake Landing (Sibitt et al. (2012)). However, there have been a few attempts to demonstrate STES on the single detached house scale. Most of these systems were designed for very low energy houses, and feature solar thermal arrays ranging from 10-42 m^2 and seasonal storage tanks ranging from 12-40 m^3. The interested reader is directed to the designs of Besant et al. (1979) and Esbensen and Korsgaard (1977), though neither present experimental results.

Colclough et al. (2011) present a STES system installed on a low energy home in Ireland. The system featured a 10.8 m^2 evacuated tube solar array, 300 litre DTES tank and a 23 m^3 STES tank. The system achieved solar fractions of 56% and 93% for space heating and domestic hot water, respectively. Heat losses from the STES tank were found to be more significant than predicted. The experimental heat loss coefficient found was approximately 10 W/K, despite calculations from nominal insulation properties giving 4.2 W/K (Clarke (2014)).

Other STES installations have shown higher heat losses than expected as well. Marazella’s XST model was validated by Raab (2005) for the STES tank in Hannover. A parameter investigation based on measured data suggested that the thermal conductivity of the granular glass STES insulation must be approximately 0.10 W/mK. This was approximately 40% higher than the value found for dry granular glass (0.072 W/mK) when measured in a lab setting. The authors attribute this to moisture migration in the insulation and thermal bridging in the tank support materials. It is clear from the literature that care should be taken when using nominal insulation properties in designing and simulating STES tanks.

3. Experimental Setup

This section provides an overview of the design of the research home and solar thermal system, as well as its instrumentation and control system. The section concludes with a brief discussion of cooldown tests commenced to determine heat loss rates in the STES tank.

3.1 The Urbandale Centre for Home Energy Research

The Urbandale Centre for Home Energy Research (CHEeR) is an experimental research house built to study various innovative home energy systems. The house, pictured in Figure 1, contains a basement and two above-ground storeys with 149 square-meters of heated floor area. The house was intended to exceed current Canadian energy standards (i.e. R-2000) but to remain realistic under current building practices. The east, west and south walls have a nominal U-value of 0.21 W/m^{2}K, while the north walls are more heavily insulated at 0.12 W/m^{2}K. The attic is freely ventilated, and contains blown-in insulation with a U-value of 0.11 W/m^{2}K. The basement slab is insulated with rigid foam board with a U-value of 0.36 W/m^{2}K, and the basement walls have a U-value of 0.21 W/m^{2}K. The building's airtightness at 50 Pa depressurization was measured to be 1.3 ac/h. Almost all of the windows are placed on the south side of house to maximize solar gains. The total south-facing window area of the house is 20 m^2. All windows are triple-glazed with an argon fill and two low-emissivity coatings.

CHEeR has several redundant heating and cooling systems. An air-source heat pump connected to rock bed heat storage can heat or cool the house. An extensive hydronic network connects an evacuated tube solar array with one of two buried seasonal stores; a large insulated sandbox and a large buried water tank. The collectors can also charge a number of smaller hot water tanks for diurnal storage and to provide DHW. The hydronic network can supply either a radiant floor or a hydronic air handler.

The house is equipped with a large suite of instrumentation. Indoor air temperatures are measured at several locations on each storey using shielded, aspirated thermocouples. On the roof sits a weather station that can measure outdoor air temperature, humidity, and wind speed. A number of pyranometers measure direct and diffuse radiation on the horizontal, vertical and collector tilt (60°) planes.

3.2 Solar Combisystem with Seasonal Storage

The solar thermal system used in this research is shown schematically in Figure 2. The solar array consists of ten Apricus AP-30 evacuated tube collectors in two parallel lines of five. The collectors face south, and are tilted at 60° to bias solar collection towards winter. An antifreeze solution consisting of 60% Intercool Biogreen and 40% water is run through the collectors to prevent freezing in winter. Actuated valves allow the solar array to charge either the diurnal storage tanks or the seasonal storage tank. The antifreeze solution indirectly charges these loads through heat exchangers.

The diurnal store consists of three insulated 450-litre tanks. The primary diurnal tank, Tank A in Figure 2, is charged through an immersed-coil heat exchanger. A circulator pump can move hot water from the primary tank (A) to the secondary and tertiary tanks (B and C). Tank A is used to supply DHW to a load mimicry system, while Tanks B and C can provide hot water to the radiant floor. The seasonal storage tank is used only for space heating, and can heat the radiant floor through a heat exchanger.

Because the research home does not have mains water connection, domestic hot water draws must be mimicked experimentally. To do this, the solar collector loop is used to cool two 450 litre "DHW mimicry" tanks overnight. Flow in the collector loop is directed through heat dissipators mounted on the northern roof of the research house, which cools the DHW tanks through a heat exchanger. To mimic draws, water is exchanged between DTES Tank A and the DHW mimicry cool tanks. Hot water draws follow a typical Canadian hot water draw schedule developed by Edwards (2015)

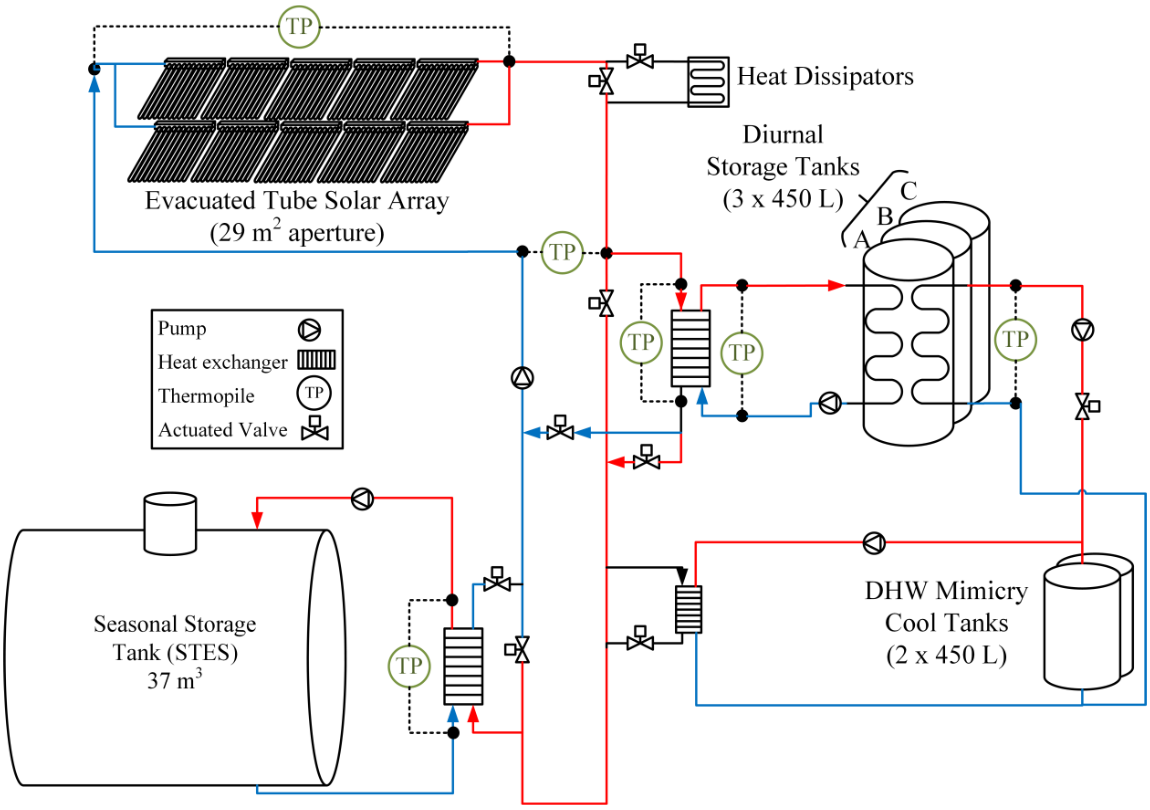

Fig. 2: Simplified schematic of CHEeR's solar thermal system with seasonal storage

The seasonal storage tank (Figure 1.b) couples to the collector loop (Fig. 2) and radiant flooring loop (not pictured) through heat exchangers. The tank is approximately 37 m^3 in volume, and features two sets of inlets and outlets for charging and discharging (Figure 3). The tank inlets and outlets were designed to promote stratification in the tank; the pipes are 10 cm in diameter to produce low flow velocities, and the inlet tubes are perforated to encourage water to reach its appropriate temperature level. The perforations are 9.5 mm in diameter and spaced 5 cm apart vertically. The tank was insulated with 30.5 cm of spray-on polyurethane insulation, which gives it a nominal U-value of 0.075 W/m^2K.

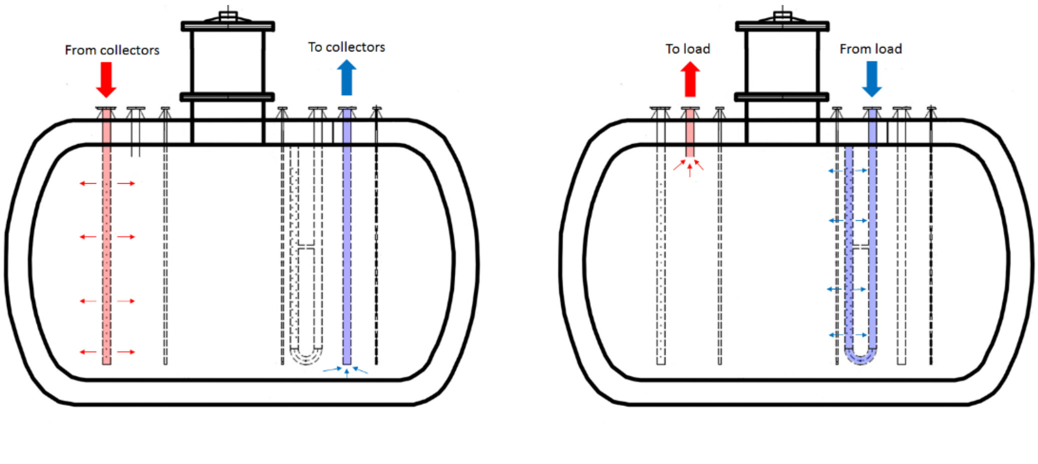

a) b)

Fig. 3: Seasonal storage tank, with a) solar charging inlet and outlet, and b) space heating inlet and outlet

The tank's access hatch is above ground. To insulate the hatch, a small structure was created. Figure 4 shows a cross-sectional view of the hatch insulating structure. Five sheets of 7.6 cm rigid foamboard (nominally RSI 2.6 each) surround the hatch on each side. The cavity formed between the foamboard and hatch is stuffed with batt insulation (not shown). The foamboard pieces are affixed to one another with adhesive spray foam. The foamboard structure is surrounded by an air barrier, which is buried under a layer of soil. The design U-value of this structure is intended to match that of the tank's insulation (0.075 W/m^{2}K).

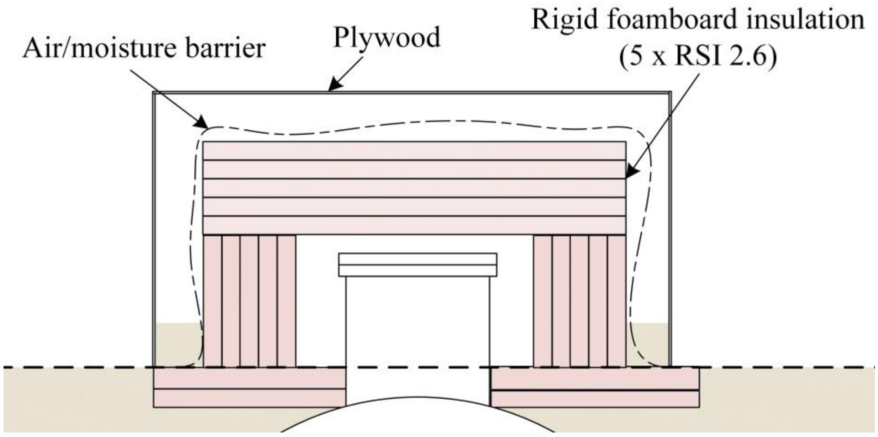

Fig. 4: Insulation of the STES access hatch

2.3 Instrumentation

We are primarily interested in measuring heat transfer rates within the solar thermal system. Heat transfer rates can be determined using the 1st law of thermodynamics and by treating the fluid (water or antifreeze) as an incompressible with constant density and specific heat:

$$\dot{Q} = (\rho c_p)\big|_T \dot{V} \Delta T \quad \text{(eq.1)}$$

Where $\dot{V}$ is volumetric flow rate and ΔT the temperature rise in the fluid. Volumetric flow rates are measured by positive displacement oval gear flowmeters, which are manufacturer-calibrated to a bias error of ±1% of reading.

Temperature differences are measured with six-junction thermopiles. An example of a typical heat transfer station is shown in Figure 5.

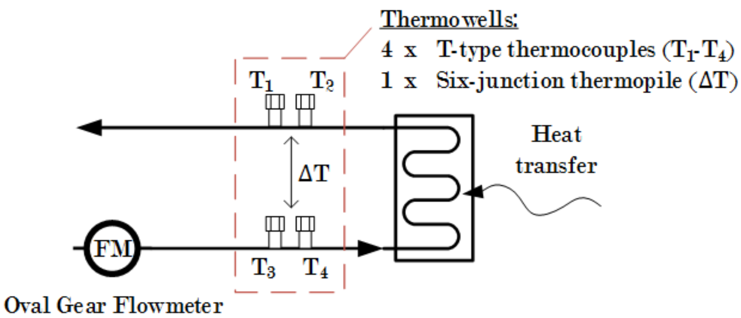

Fig. 5: Example of instrumentation on a heat transfer station

The thermopiles were calibrated using highly accurate platinum RTDs, and the bias error was calculated according to the methods detailed by Moffatt (1988) considering all sources of error. This included the voltage reading error of the data acquisition system, curve-fitting errors, and the bias error of the platinum RTDs themselves. Assuming negligible uncertainty is associated with material properties (density, specific heat), the total bias error for heat flows is less than 2% for temperature differences of 3°C and above. Some (but not all) thermopiles are shown on Figure 2. Eleven heat flows are monitored in total.

Stratification and heat loss performance of the seasonal storage tank can be inferred from three vertical racks of

25 T-Type thermocouples (Figure 3) that are immersed along the tank's vertical mid-plane. As with the thermopiles, a calibration was performed on the thermocouples. The bias error associated with a single thermocouple measurement was found to be 0.45°C when all sources of bias were considered.

2.4 Controls

The control scheme for the solar thermal system was designed to be similar to Wills (2013) and Kemery (2017). While it is almost certainly non-ideal, it was selected for its simplicity and ease of implementation in preliminary experimentation. Future work will examine optimum control configurations, for instance, the use of variable speed pumps to increase collector temperatures during low irradiance. The control algorithm is written in NI LabVIEW (National Instruments, (2017)) which runs in real-time on three NI data acquisition (DAQ) systems, which in turn actuate the pumps and valves in the system.

The control scheme for solar charging is given in Figure 6. When a given level of solar irradiation on the collector plane or sufficient collector temperature is sensed, the solar collector pump is triggered. If hot enough to charge the loads in the system (i.e. the collector outlet temperature T_{coll} exceeds the load temperature plus the "on" setting ΔT_{ON}), the algorithm selects a load to charge based on a pre-set priority list. The highest priority load is DTES Tank A. The tank is maintained at a set point T_{DHW} so that it can always supply domestic hot water. When charged in heating season, DTES B and C are prioritized over the seasonal store. If the system is charging the DTES, the temperature of the antifreeze after the DTES heat exchanger is sensed to see if it exceeds the mean seasonal store temperature. If so, the seasonal store is charged in series with the DTES. If the collector temperature falls below a certain level (determined by the load temperature plus setting ΔT_{OFF}), the solar pump is shut off.

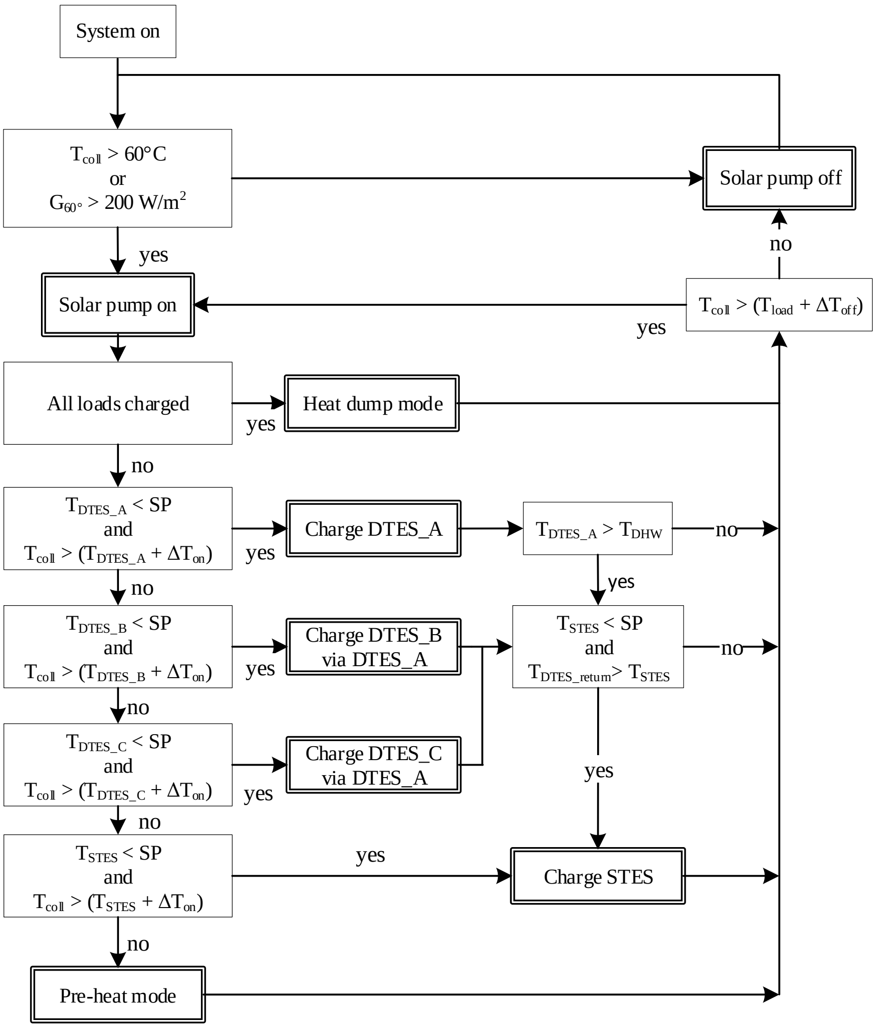

Fig. 6: Control strategy for charging the solar thermal system

A description of the control variables mentioned in Figure 6 are given in Table 1.

Tab. 1: Description of solar control parameters

Variable	Setting
T_{coll}	Temperature determined by an RTD placed on the solar collector
$G_{60°}$	Solar irradiance measured by a pyranometer on the collector plane
SP	Set point
T_{DTES_i}, T_{STES}	Temperature of a diurnal tank *i*, temperature of the seasonal storage tank
T_{load}	Temperature corresponding to the current load being charged

3.4 Cooldown Tests

The ability of the seasonal storage to preserve thermal energy has obvious implications on its yearly performance. Two cooldown tests of the seasonal store, performed in July of 2016 and 2017 respectively, show early indications of the tank's heat loss performance. During the cooldowns, solar charging of the tank was ceased so that all energy transfer could be attributed to heat losses. The temperature distribution in the tank was then monitored over 2-3 weeks. During the July 2016 test, the tank began the test well-mixed at an average temperature of 72.2°C, while in 2017 the tank began approximately 5°C hotter at the top than bottom with an average temperature of 63.6°C. The results of these tests are given in the next section.

4. Results

Cooldown results for both tests are given in Figure 7. Results are given for the average temperature of 5 stratums within the tank, each containing 5 thermocouples (S1 through S5) from each of the three thermocouple racks. No significant temperature differences were found between the three thermocouple racks in the tank.

For the well-mixed test, the average heat loss rate was 530 W. No development of natural stratification due to heat loss is apparent during this time, and similar heat loss rates are seen in all layers of the tank. The stratified cooldown shows accelerated temperature loss at the top and bottom of the tank (S1, S5) relative to the middle layers. Destruction of stratification can be seen as layers S2 through S5 converge to a similar temperature around 300 hours. However, the bottom layer of the tank remained 5°C below the top layer throughout the test. The average late of heat loss for this test was approximately 350 W.

In both test cases, measured heat loss rates exceed expected values. According to Kemery (2016), even if a conservative ground temperature of 10°C is assumed, heat loss rates for a 72°C tank with 0.075 W/m^2K insulation should not exceed about 285 W. It is possible that these higher than expected losses are the result of heat loss from the tank's above-ground access hatch. It should be noted that during the 2016 tests, the foamboard sheets used to insulate the hatch did not extend underground as shown in Figure 4. Instead, they simply sat on the ground surface. The air barrier was also not installed until 2017. Hatch losses would not explain higher than expected losses from the bottom layer of the tank. Moisture migration in insulation is a typical cause for greater than expected losses, but this is deemed unlikely, as product specifications show the spray-foam insulation to be unaffected by moisture content. Further, the tank has a double-wall construction that should prevent moisture migration. Thermal bridges within the insulation are another possible explanation. Thermal bridges could be caused by either structural members within the tank or non-uniformities in the insulation coverage.

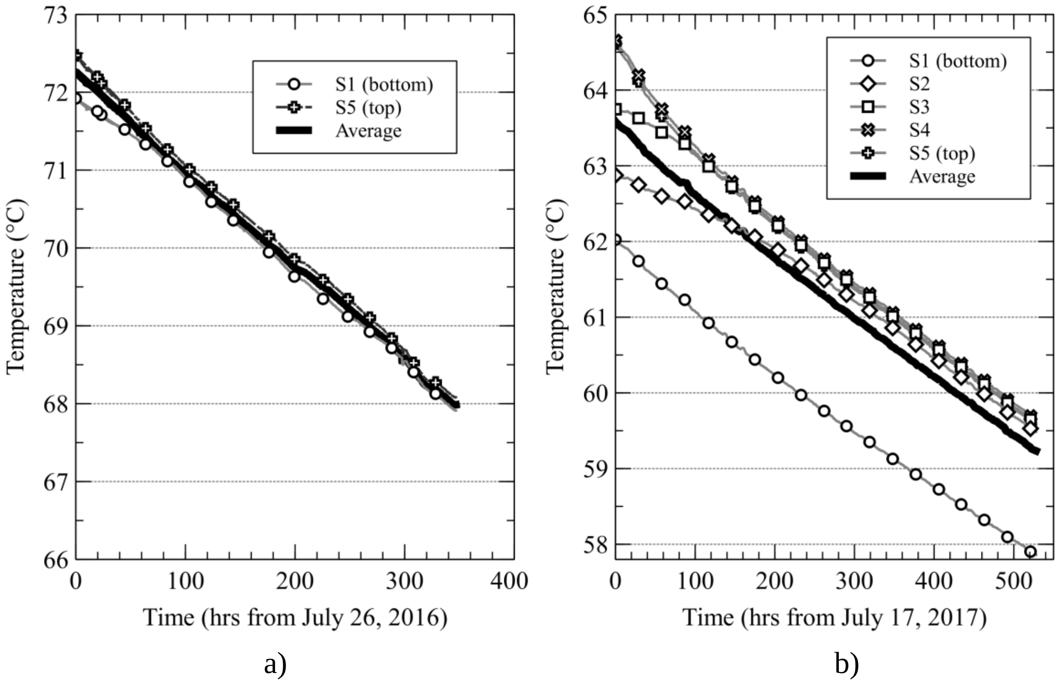

Fig. 7: Temperature loss during seasonal storage cooldowns with a) well-mixed and b) 5°C stratified starting conditions

Regardless, as evidenced by the work of Colclough (2011) and Raab (2005) referenced earlier in this paper, excess losses appear to be a common trend with buried STES tanks, and may not indicate poor performance for the combisystem. Kemery (2016) performed a sensitivity study wherein the ground temperature was varied from 5 to 25°C. The ground temperature was used as a constant boundary temperature for the seasonal store. Simulation results showed that the solar thermal system's performance was not particularly sensitive to heat losses. This might be explained by the relatively high ratio of collector area to storage volume at CHEeR; lost heat can be quickly recovered by the large array. However, even with an imposed 5°C boundary temperature, predicted heat losses were less than those found through experiment. Predicted losses ranged from 6.9 to 9.5 GJ yearly. If we consider the experimental heat loss tests to represent typical average losses for the year, approximately 11 to 17 GJ of heat would be lost from the as-built tank yearly. That would represent 16 to 28% of the total solar energy collected by the solar array, based on Kemery's estimation of 60-70 GJ collected yearly. It should be noted that at the time of writing, the seasonal storage tank has only undergone one full annual charge and discharge cycle. It is possible that the surrounding ground is still in a transient state; that is, heat losses from the tank could be reduced as the ground warms up. Kemery (2016) notes that 4 years of simulation were required before the STES system reached a consistent cyclical behavior.

5. Conclusions and Future Work

This paper has presented an overview of the design of a solar combisystem with seasonal thermal energy storage. The system's components, instrumentation and control system were described. Preliminary results from heat loss tests show that the seasonal storage tank loses heat at faster rate than would be expected based on nominal properties of the insulation. Explanations for larger than expected losses are postulated, including losses through the access hatch and thermal bridging.

Future work will quantify the energy performance of the solar combisystem over a full heating and cooling season. A model of the as-built seasonal storage tank will be developed and validated in TRNSYS software (Thermal Energy Storage Specialists (2017)), and coupled to a full building model of the CHEeR house in ESP-r (Energy Systems Research Unit, University of Strathclyde (2017)), following the work of Wills (2013) and Kemery (2016). Parametric studies will re-examine the sizing and control of the solar combisystem, and multi-objective optimization will be performed for system performance and economic consideration.

6. References

Besant, R., Dumont, R., and Schoenau, G., 1979. The Saskatchewan conservation house: Some preliminary performance results. Energy and Buildings, 2(2):163-174

Braun, J., Klein, S. and Mitchell, J., 1981. Seasonal storage of energy in solar heating. Solar Energy, 26(5):403-411.

Clarke, J., Colclough, S., Griffiths, P., and McLeskey Jr., J.T., 2014. A Passive House with Seasonal Solar Energy Store: In Situ Data and Numerical Modeling, International Journal of Ambient Energy, 35(1): 37-50.

Colclough, S., Grihs, P., and Hewitt, N.,2011. A year in the life of a passive house with solar energy store. In Energy Storage Conference, (Belfast, Ireland), IC-SES.

Dincer, I. and Rosen,M., 2011 Thermal Energy Storage: Systems and Applications, second ed. John Wiley & Sons, Hoboken, NJ, USA.

Edwards, S., 2014. Sensitivity Analysis of Two Solar Combisystems Using Newly Developed Hot Water Draw Profiles. M.A.Sc Thesis, Carleton University.

Edwards, S., Beausoleil-Morrison, I., and Laperriere, A., 2015. Representative hot water draw profiles at high temporal resolution for simulating the performance of solar thermal systems. Solar Energy, vol 111, pp.43-52.

Esbensen, T. and Korsgaard, V., 1977. Dimensioning of the solar heating system in the zero energy house in Denmark. Solar Energy, 19(2):195-199.

ESP-r, 2017. Energy Systems Research Unit, University of Strathclyde, Accessible online at http://www.esru.strath.ac.uk/Programs/ESP-r.htm.

Kemery, B., 2017. Analysis and design of a solar-combisystem for high solar fraction Canadian housing with diurnal and seasonal water-based thermal stores, M.A.Sc. thesis, Carleton University.

LabVIEW, 2015. Version 15.0. National Instruments.

Marazella, L., 1992. Multi–flow stratified thermal storage model with full–mixed layers PdM-XST. Technical report., University of Stuttgart and Dipartimento di Energetica Politecnico di Milano.

Moffat, R., 1988. Describing the uncertainties in experimental results. Experimental Thermal and Fluid Science, 1(1):3-17.

Ochs, F., 2009. Modeling large-scale thermal energy stores. Ph.D. thesis, University of Stuttgart.

Pinel, P., Cruickshank, C., Beausoleil-Morrison, I. and Wills,A., 2011. A review of available methods for seasonal storage of thermal energy in residential applications. Renewable and Sustainable Energy Reviews, 15(7): pp. 3341-3359.

Raab, S., Mangold, D. and M¨uller-Steinhagen, H., 2005. Validation of a computer model for solar assisted district heating systems with seasonal hot water heat store. Solar Energy 79(5): 531–543.

Sibbitt, B., McClenahan, D., Djebbar, R,. Thornton, J., Wong, B., Carriere, J. And Kokko, J., 2012. The performance of a high solar fraction seasonal storage district heating system - five years of operation. Energy Procedia, 30:856-865.

Sillman, S., 1981. Performance and economics of annual storage solar heating systems. Solar Energy, 27(6):513-528.

TRNSYS, 2017. A Transient System Simulation Program, Version 17, Thermal Energy System Specialists.

Wills, A., 2013. Design and co-simulation of a seasonal solar thermal system for a Canadian single-family detached house. M.A.Sc. thesis, Carleton University.